ARTICLE NO. 80-4071

Deadbeat Nutation Controller for Momentum Bias Stabilized Spacecraft

J. S.-C. Yuan*
Spar Aerospace Limited, Toronto, Canada

A control procedure is presented for the deadbeat control of nutation in a one-axis momentum bias stabilization system. Nutation as well as attitude errors are brought to zero in finite time via a sequence of two control impulses. At the same time, the total control torque impulse is minimized subject to predefined constraints on the impulse size and bounds on the attitude errors. Being algorithmic, the controller is particularly suited for microcomputer implementation. In principle, any degree of control accuracy may be achieved through the definition of an appropriate "deadzone" in the control algorithm. The design flexibility of the proposed controller greatly surpasses that of the conventional pseudorate controller.

Nomenclature

a_1, a_3 = parameters defined in Eqs. (39) and (40)
$B(\cdot)$ = boundary of a set
c, d, f = parameters defined in Eqs. (35-37)
D = deadzone in roll-yaw plane [see Eq. (45)]
G = error constrained control torque impulses [see Eq. (50)]
h = momentum bias
H, H_1-H_6 = amplitude constrainted control torque impulses [see Eqs. (43) and (44)]
i = $\sqrt{-1}$
I_1, I_3 = roll and yaw moments-of-inertia
I = $\sqrt{I_1 I_3}$
J = sum of squared control torque impulses [see Eq. (51) or Eq. (52)]
K = unconstrained deadbeat control torque impulses [see Eq. (41)]
M = line in (ϕ, ψ) plane defined in Eq. (27)
P_0, Q_0 = coefficients of unforced nutation motion [see Eqs. (11) and (12)]
P, Q = coefficients of forced nutation motion [see Eqs. (13) and (14)]
P' = P due to second control impulse [see Eq. (23) or (33)]
r, s = coordinates of $(P_0 + P)$ defined in Eqs. (47-49)
t^* = deadbeat time [see Eq. (38)]
T_1, T_3 = external torques about roll and yaw axes
u = normalized complex external torque [see Eq. (7)]
x, x' = first and second torque impulses (complex)
x_1, x_1' = first and second torque impulses (real) of offset thrusters
x_3, x_3' = first and second torque impulses (real) of yaw thrusters
x_1^*, x_3^* = unconstrained optimal deadbeat control torque impulses [see Eqs. (54) and (55)]
x_{1m}, x_{3m} = *amplitude bounds on control torque impulses*
z = $\phi + i\psi$
$z_0, \dot{z}$ = $z(0)$, $\dot{z}(0)$ [see Eq. (9)]
α = thruster offset angle [see Fig. 1]
$\delta(\cdot)$ = Dirac function
ϵ = set membership
ϕ, ψ = Euler's roll and yaw angles
ϕ_0, ψ_0 = $\phi(0), \psi(0)$
$\dot{\phi}_0, \dot{\psi}_0$ = $\dot{\phi}(0), \dot{\psi}(0)$
ϕ_{db}, ψ_{db} = roll and yaw deadbands
ω_1, ω_3 = angular rates about roll and yaw axes
ω_0 = orbit rate
ω_n = nutation frequency [see Eq. (3)]

Received June 26, 1979; revision received Nov. 20, 1979.

Index categories: Analytical and Numerical Methods; Spacecraft Dynamics and Control.

*Senior Engineer. Member AIAA.

Introduction

EVER since its introduction, the WHECON (acronym for "wheel control") concept[1] has been widely used in a variety of three-axis stabilized spacecraft; one of the more recent ones is the Communications Technology Satellite (CTS). In this concept, a momentum wheel is aligned along one of the spacecraft axes, providing gyroscopic stiffness about the remaining two axes. A distinct advantage of this concept is that the errors in the latter two axes are coupled via the gyrocompassing effect. This means error sensing is required in only one of the two axes. In a body-fixed reference system, the wheel momentum vector is aligned along the pitch axis which is nominally perpendicular to the equatorial orbit plane. The roll axis is directed along the orbital velocity vector, and the yaw axis is pointed at the Earth center. Only the pitch and roll errors are sensed.

The nutational motion is damped by correction torques provided by a pair of thrusters whose torque vector is offset in the roll-yaw plane. The thrusters are conventionally actuated by a pseudorate controller[1-3] which provides the necessary closed-loop phase lead for nutation damping. Control accuracy is determined by the deadband in the controller. Because nutation is not completely damped, additional control augmentation is usually required in order to prevent limit-cycle operation in the deadband. The control accuracy of such a system is typically in the range of ± 0.1 to ± 0.5 deg.[4]

Future communications satellites, however, will require significantly higher pointing accuracy. Typically, accuracies of ± 0.05 deg in roll and pitch, and ± 0.2 deg in yaw are regarded as the design goal. The stringent pointing accuracy requirements will demand upgrading the performance of the current momentum bias control system. In particular, the tight roll and yaw error margins indicate that direct yaw sensing and control may be necessary, especially during periods of large disturbances such as stationkeep and momentum dump.

Yaw estimation has been studied in a number of recent works[5-7] and will not be treated here. Recent efforts at improving the pointing accuracy of the momentum bias system have included the addition of a yaw control loop to the WHECON system.[8] However, the pointing accuracy is still

severely limited by the choice of parameters in the pseudorate controllers. An alternative approach[9] involves the use of a yaw momentum wheel which, in effect, results in a two-axis momentum bias system. The improved accuracy is achieved only at the expense of an additional wheel.

This paper presents a novel approach to active nutation damping for a one-axis momentum bias system by deadbeat controlling the attitude errors. There is no need for the two-tier control structure that is used for large-angle and deadband operations in the conventional pseudorate controller. Indeed, the concept differs significantly from the pseudorate control approach in that the controller is mainly algorithmic; hence, it is best suited for implementation in an on-board processor. Being free from hardware limitation, the definition of "deadzone" is entirely arbitrary. In principle, any degree of control accuracy may be achieved.

Problem Formulation

A general single-axis momentum bias system is described in Fig. 1. At sufficiently small angular rates, the roll and yaw dynamics may be decoupled from the pitch motion and written as

$$I_1\dot{\omega}_1 + h\omega_3 = T_1 \tag{1}$$

$$I_3\dot{\omega}_3 - h\omega_1 = T_3 \tag{2}$$

where I_1 and I_3 are the moments-of-inertia about the roll and yaw axes, respectively, and h denotes the momentum bias of the pitch wheel. The external torques acting about the roll and yaw axes are denoted by T_1 and T_3, respectively. In the absence of external torques, any nonzero angular rates will generate simple harmonic oscillations at a frequency given by

$$\omega_n = h/\sqrt{I_1 I_3} \triangleq h/I \tag{3}$$

This oscillation results in nutational motion of the momentum bias vector about the nominal spin axis.

For small errors in roll (ϕ) and yaw (ψ), the following approximations hold:

$$\omega_1 \simeq \dot{\phi} - \omega_0\psi \tag{4}$$

$$\omega_3 \simeq \dot{\psi} + \omega_0\phi \tag{5}$$

where ω_0 denotes the orbital rate of the spacecraft. Substitution into Eqs. (1) and (2) with the assumption

$$I_1 \simeq I_3 \simeq I$$

yields

$$\begin{bmatrix} \ddot{\phi} \\ \ddot{\psi} \end{bmatrix} + \begin{bmatrix} 0 & \omega_n - \omega_0 \\ \omega_0 - \omega_n & 0 \end{bmatrix} \begin{bmatrix} \dot{\phi} \\ \dot{\psi} \end{bmatrix} + \omega_0\omega_n \begin{bmatrix} \phi \\ \psi \end{bmatrix} = \begin{bmatrix} T_1/I \\ T_3/I \end{bmatrix} \tag{6}$$

Adopting the complex variable notation

$$z \triangleq \phi + i\psi \qquad u \triangleq (T_1 + iT_3)/I \tag{7}$$

we can simplify Eq. (6) into

$$\ddot{z} = (\omega_n - \omega_0)i\dot{z} - \omega_0\omega_n z + u \tag{8}$$

where the initial conditions are denoted by

$$z_0 = \phi_0 + i\psi_0 \qquad \dot{z}_0 = \dot{\phi}_0 + i\dot{\psi}_0 \tag{9}$$

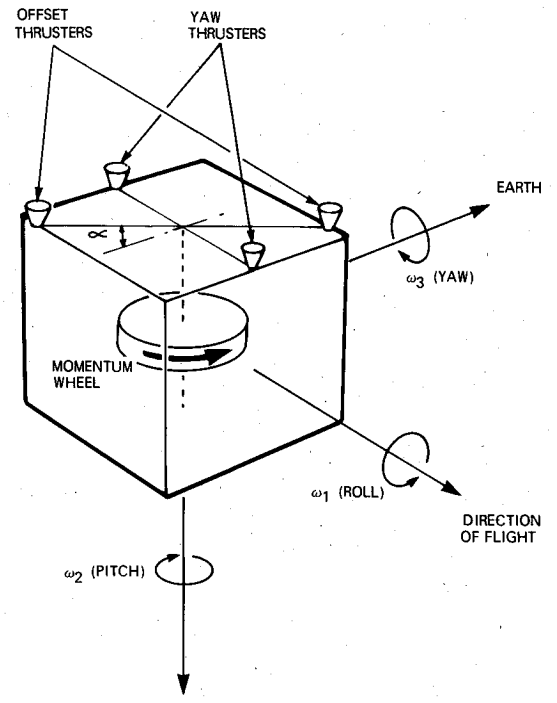

Fig. 1 A single-axis momentum bias stabilization system.

The general solution to Eq. (8) is given by

$$z(t) = [P_0 + P(t)]e^{i\omega_0 t} + [Q_0 + Q(t)]e^{i\omega_n t} \tag{10}$$

where

$$P_0 \triangleq (\omega_n z_0 + i\dot{z}_0)/(\omega_0 + \omega_n) \tag{11}$$

$$Q_0 \triangleq (\omega_0 z_0 - i\dot{z}_0)/(\omega_0 + \omega_n) \tag{12}$$

$$P(t) \triangleq \left[\frac{i}{\omega_0 + \omega_n}\right]\int_0^t e^{i\omega_0 s}u(s)\,ds \tag{13}$$

$$Q(t) \triangleq \left[\frac{-i}{\omega_0 + \omega_n}\right]\int_0^t e^{-i\omega_n s}u(s)\,ds \tag{14}$$

A few general facts about the nutation solution Eq. (10) are noted as follows:

Fact 1:

$$P_0 + Q_0 = z_0 \tag{15}$$

Fact 2: At $u(t) = 0$,

$$z(t) = P_0 e^{-i\omega_0 t} + Q_0 e^{i\omega_n t} \tag{16}$$

which describes a circle in the (ϕ,ψ) or z-plane (Fig. 2). The center of the circle rotates about the origin as a result of the orbital motion of the spacecraft.

Fact 3: Consider an impulsive torque

$$u(t) = x\delta(t)/I$$

where $\delta(\cdot)$ is the Dirac function, and x (possibly a complex variable) denotes the torque impulse. From Eqs. (13) and (14), we then have

$$P = -Q = ix/I(\omega_0 + \omega_n) \tag{17}$$

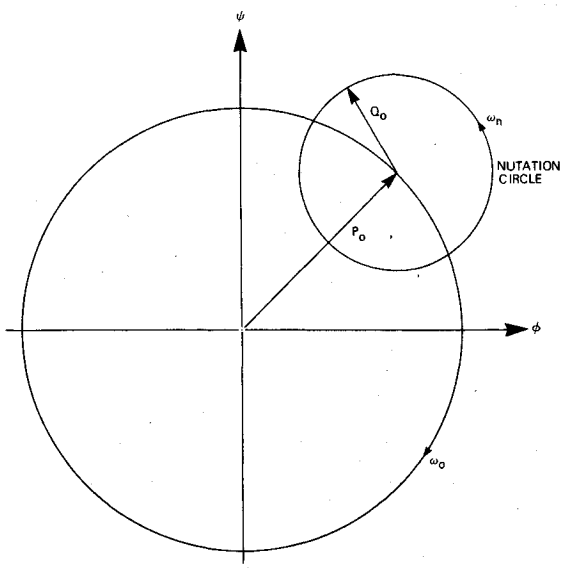

Fig. 2 Nutation in the absence of external torques.

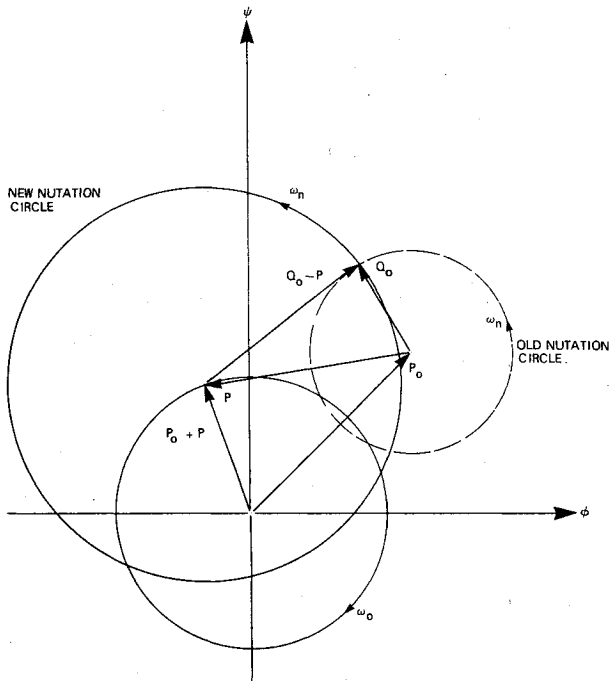

Fig. 3 Nutation induced by impulsive torques.

so that

$$z(t) = (P_0+P)e^{-i\omega_0 t} + (Q_0-P)e^{i\omega_n t} \tag{18}$$

Hence, the torque impulse has effectively shifted the center of the nutation circle via the vector P (Fig. 3). The radius of the new nutation circle is given by $\|Q_0-P\|$.

We define *deadbeat nutation damping* (DND) as the case where $z_0 \neq 0$ and

$$z(t) = 0 \qquad (t \geq t^*) \tag{19}$$

for some finite t^*. Note that as well as nutation, the total attitude errors are also reduced to zero. In this paper, we shall only be concerned with DND using impulsive torques so that the results will be directly applicable to momentum bias systems actuated by thrusters.

Synthesis Procedure for Deadbeat Nutation Control

The general requirements for DND will be discussed here. These conditions will then lead to a concrete procedure for the synthesis of DND control.

We first prove what may be intuitively obvious, namely, that DND in one control impulse is not possible.

Proposition 1: If $z_0 \neq 0$ and z is generated by a single control impulse as in Eq. (18), then there exists no finite t^* such that

$$z(t) = 0 \qquad (t \geq t^*) \tag{20}$$

Proof: We prove by contradiction. Suppose $z_0 \neq 0$ and Eq. (20) holds for some finite t^*. Then, by Eq. (18),

$$(P_0+P)e^{-i\omega_0 t} = -(Q_0-P)e^{i\omega_n t} \qquad (t \geq t^*) \tag{21}$$

Also, since $\dot{z}(t) = 0$ for $t \geq t^*$,

$$i\omega_0(P_0+P)e^{-i\omega_0 t} = i\omega_n(Q_0-P)e^{i\omega_n t} \qquad (t \geq t^*) \tag{22}$$

Combining Eqs. (21) and (22), we get

$$P_0+P=0 \qquad Q_0-P=0$$

which implies $P_0+Q_0=z_0=0$. This completes the proof.

DND is nevertheless possible if more than one control impulse is permitted, as the next result will demonstrate.

Proposition 2: Consider two control impulses separated by time $t^*>0$:

$$u(t) = x\delta(t)/I$$

$$u'(t) = x'\delta(t-t^*)/I$$

Define, as in Eq. (17),

$$P \triangleq ix/I(\omega_0+\omega_n) \qquad P' \triangleq ix'/I(\omega_0+\omega_n) \tag{23}$$

Then, $z(t)=0$, $t \geq t^*$ if and only if the following conditions hold for (P, t^*, P'):

$$\|P_0+P\| = \|Q_0-P\| \tag{24}$$

$$(P_0+P)e^{-i\omega_0 t^*} + (Q_0-P)e^{i\omega_n t^*} = 0 \tag{25}$$

$$P' + (P_0+P)e^{-i\omega_0 t^*} = 0 \tag{26}$$

Proof: We note from Eq. (18) that Eqs. (24) and (25) both follow when $z(t^*)=0$; condition (25) is both necessary and sufficient. Also, by Eq. (25)

$$\dot{z}(t^*) = -i(\omega_0+\omega_n)(P_0+P)e^{-i\omega_0 t^*}$$

When $z(t^*)=0$, $z(t)$ for $t>t^*$ is given by

$$z(t-t^*) = \left[\frac{i\dot{z}(t^*)}{(\omega_0+\omega_n)} + P'\right][e^{-i\omega_0(t-t^*)} - e^{i\omega_n(t-t^*)}]$$

$$= [(P_0+P)e^{-i\omega_0 t^*} + P'][e^{-i\omega_0(t-t^*)} - e^{i\omega_n(t-t^*)}]$$

which is zero if and only if Eq. (26) holds.

Thus, the DND controller is completely characterized by the parameters (P, t^*, P'), or equivalently, (x, t^*, x'). The practical value of Proposition 2 is that the conditions (24-26) in fact constitute a design procedure for these control parameters.

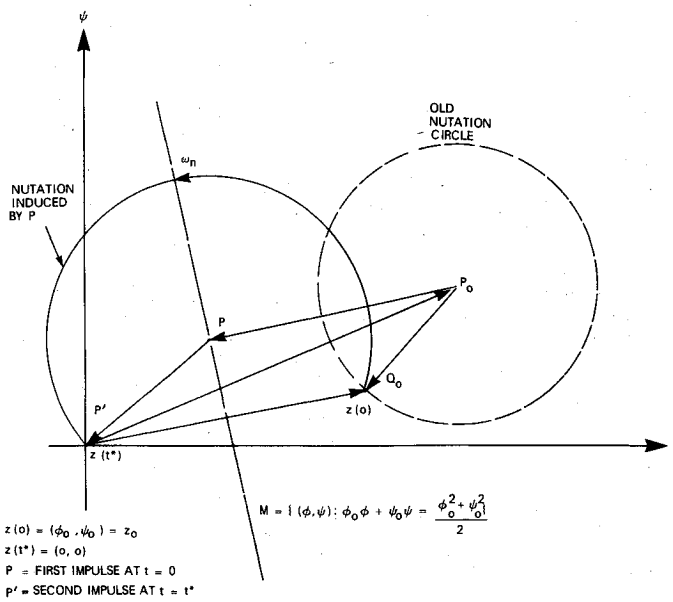

Fig. 4 Deadbeat nutation damping in two control impulses.

Obviously, other multipulse DND solutions also exist. In this paper, we shall confine our attention to the class of two-impulse solutions, as it is also important in practice to prolong the thruster life by minimizing the number of control pulses.

A geometrical interpretation of the two-impulse DND solution is as follows (cf. Fig. 4). The locus of all the points in the z-plane which are equal in distance from z_0 and from the origin is given by the line

$$M \triangleq \{(\phi,\psi): \quad \phi_0\phi+\psi_0\psi = \tfrac{1}{2}(\phi_0^2+\psi_0^2)\} \tag{27}$$

which orthogonally bisects the vector z_0. From Fact 3, we note that the nutation circle induced by the first impulse is centered at P_0+P, and has radius $\|Q_0-P\|$. Hence, providing that

$$P_0+P \in M \tag{28}$$

the nutation circle will pass through the origin, and condition (24) is automatically satisfied. Along the path of any such nutation circle, z will pass the origin within one nutation period. At the time t^* when z reaches the origin, the second impulse given by

$$P' = -(P_0+P) \tag{29}$$

will then generate a nutation circle centered at the origin with zero radius, in effect, resulting in DND.

With P given by Eq. (24) or Eq. (28), the deadbeat time t^* may be computed from Eq. (25). Furthermore, Eq. (28) ensures that $t^* < 2\pi/\omega_n \ll 2\pi/\omega_0$, so that Eq. (29) may also be obtained from Eq. (26) by setting $\exp(-i\omega_0 t^*)$ to one.

To illustrate the use of Eqs. (24-26) as a design tool, let us consider the case where the control torques are provided by a pair of roll-yaw thrusters offset at angle α together with a pair of yaw thrusters (cf. Fig. 1). The thrusters are pulsed simultaneously so that

$$u(t) = \{[x_1\cos\alpha + i(x_3 - x_1\sin\alpha)]/I\}\delta(t) \tag{30}$$

where x_1 and x_3 denote the torque impulses generated by the offset and the yaw thrusters, respectively. Similarly, we denote the control torque impulses at time t^* by x_1' and x_3' and write

$$u'(t) = \{[x_1'\cos\alpha + i(x_3' - x_1'\sin\alpha)]/I\}\delta(t-t^*) \tag{31}$$

So, as in Eq. (23), we have

$$P = [x_1(\sin\alpha + i\cos\alpha) - x_3]/I(\omega_0+\omega_n) \tag{32}$$

$$P' = [x_1'(\sin\alpha + i\cos\alpha) - x_3']/I(\omega_0+\omega_n) \tag{33}$$

The DND solution now consists of the parameter set $\{x_1, x_3, t^*, x_1', x_3'\}$. Indeed, we shall show presently that (t^*, x_1', x_3') are uniquely determined by x_1 and x_3 so that a DND solution simply comprises the pair (x_1, x_3).

By substituting terms in P_0, Q_0, and P from Eqs. (11), (12), and (32), respectively, into Eq. (24), we get the simple relationship

$$cx_1 + dx_3 = f \tag{34}$$

where

$$c \triangleq \phi_0\sin\alpha + \psi_0\cos\alpha \tag{35}$$

$$d \triangleq -\phi_0 \tag{36}$$

$$f \triangleq I\{(\phi_0\dot{\psi}_0 - \psi_0\dot{\phi}_0) + (\omega_0-\omega_n)(\phi_0^2+\psi_0^2)/2\} \tag{37}$$

Consequently, the time t^* may be obtained from Eq. (25) as

$$t^* = \left\{\tan^{-1}\left[\frac{x_1\cos\alpha + I(\omega_n\psi_0+\dot{\phi}_0)}{x_1\sin\alpha - x_3 + I(\omega_n\phi_0-\dot{\psi}_0)}\right] - \tan^{-1}\left[\frac{x_1\cos\alpha - I(\omega_0\psi_0-\dot{\phi}_0)}{x_1\sin\alpha - x_3 - I(\omega_0\phi_0+\dot{\psi}_0)}\right]\right\} \times (\omega_0+\omega_n)^{-1} \tag{38}$$

where x_1 and x_3 both satisfy Eq. (34). For $\omega_0 \ll \omega_n$, we replace Eq. (26) with Eq. (29) and obtain

$$x_1 + x_1' = -I(\omega_n\psi_0 + \dot{\phi}_0)/\cos\alpha \triangleq a_1 \tag{39}$$

$$x_3 + x_3' = I\{\omega_n\phi_0 - \dot{\psi}_0 - \tan\alpha(\omega_n\psi_0+\dot{\phi}_0)\} \triangleq a_3 \tag{40}$$

from which x_1' and x_3' may be computed. The DND solution is thus complete.

Since x_1', x_3', and t^* are uniquely defined by x_1 and x_3 through Eqs. (38-40), a complete DND solution thus consists only of the solution to the linear equation (34). In the (x_1, x_3) plane, these solutions may be represented by the line

$$K \triangleq \{(x_1,x_3): \quad cx_1 + dx_3 = f\} \tag{41}$$

Clearly, without further constraints on (x_1, x_3), the number of such solutions is infinite.

Control Constraints

Constraints on the control torque impulses (x_1, x_3) do exist in practice. Two of the more common types are 1) minimum impulse size, and 2) attitude error bounds.

The minimum impulse constraints result from the minimum on-time requirement in most jet thrusters. For our purpose, it suffices to express the bounds as

$$|x_i| \geq x_{im} \qquad |x_i'| \geq x_{im} \qquad (i=1,3) \tag{42}$$

By Eqs. (39) and (40), the second inequality is equivalent to

$$|a_i - x_i| \geq x_{im} \qquad (i=1,3)$$

In addition, we also allow $x_i = 0$ or $x_i' = 0$. The points in the (x_1, x_3) plane that satisfy the impulse constraints (42) may then be grouped into a set

$$H \triangleq \bigcup_{i=0}^{6} H_i \tag{43}$$

where

$$H_0 \triangleq \{(x_1,x_3):\ |x_i| \geq x_{im},\ |a_i - x_i| \geq x_{im},\ (i=1,3)\}$$

$$H_1 \triangleq \{(x_1,x_3):\ x_1 = 0,\ |a_1| \geq x_{1m},\ |x_3| \geq x_{3m},\ |a_3 - x_3| \geq x_{3m}\}$$

$$H_2 \triangleq \{(x_1,x_3):\ x_3 = 0,\ |a_3| \geq x_{3m},\ |x_1| \geq x_{1m},\ |a_1 - x_1| \geq x_{1m}\}$$

$$H_3 \triangleq \{(x_1,x_3):\ x_1 = a_1,\ |a_1| \geq x_{1m},\ |x_3| \geq x_{3m},\ |a_3 - x_3| \geq x_{3m}\}$$

$$H_4 \triangleq \{(x_1,x_3):\ x_3 = a_3,\ |a_3| \geq x_{3m},\ |x_1| \geq x_{1m},\ |a_1 - x_1| \geq x_{1m}\}$$

$$H_5 \triangleq \{(x_1,x_3):\ x_1 = a_1,\ |a_1| \geq x_{1m},\ x_3 = 0,\ |a_3| \geq x_{3m}\}$$

$$H_6 \triangleq \{(x_1,x_3):\ x_3 = a_3,\ |a_3| \geq x_{3m},\ x_1 = 0,\ |a_1| \geq x_{1m}\} \tag{44}$$

The impulse constrained DND solutions are thus given by the set $K \cap H$.

Constraints on the attitude errors arise from the need to maintain the nutation circle induced by the first control impulse within reasonable bounds. We define a deadzone in the z-plane by

$$D \triangleq \{(\phi,\psi):\ |\phi| < \phi_{db},\ |\psi| < \psi_{db}\} \tag{45}$$

so that if $z_0 \in D$, no control action is taken. The roll and yaw deadbands (ϕ_{db}, ψ_{db}) thus determine the accuracy of the DND controller. For $z_0 \notin D$, we define the following bounds on $(\phi(t),\psi(t))$ for $0 \leq t \leq t^*$:

$\phi_0, \psi_0 \geq 0$:

$$-\phi_{db} \leq \phi(t) \leq \phi_0 \qquad 0 \leq \psi(t) \leq \max\{\psi_{db}, \psi_0\} \tag{46a}$$

$\phi_0 \leq 0, \quad \psi_0 \geq 0$:

$$\min\{\phi_0, -\phi_{db}\} \leq \phi(t) \leq 0 \qquad -\psi_{db} \leq \psi(t) \leq \psi_0 \tag{46b}$$

$\phi_0, \psi_0 \leq 0$:

$$\phi_0 \leq \phi(t) \leq \phi_{db} \qquad \min\{\psi_0, -\psi_{db}\} \leq \psi(t) \leq 0 \tag{46c}$$

$\phi_0 \geq 0, \quad \psi_0 \leq 0$:

$$0 \leq \phi(t) \leq \max\{\phi_0, \phi_{db}\} \qquad \psi_0 \leq \psi(t) \leq \psi_{db} \tag{46d}$$

Satisfaction of these bounds ensures that the nutation errors induced by the control impulses will be "reasonable" in size—in particular, when z_0 is on the boundary of D, $z(t) \in D$ for $0 \leq t \leq t^*$.

It is necessary to convert Eqs. (46) into an equivalent set of constraints on (x_1, x_3). We note from Fig. 4 that at any starting point z_0, the nutation circle induced by the first control impulse is determined uniquely by the position of its center $(P_0 + P)$. Hence, the attitude constraints (46) may be translated into a set of constraints on the coordinates of $(P_0 + P)$.

From Eqs. (11) and (32), we can write

$$P_0 + P = r(x_1,x_3) + is(x_1) \tag{47}$$

where

$$r(x_1,x_3) \triangleq \{I(\omega_n \phi_0 - \dot{\psi}_0) + x_1 \sin\alpha - x_3\}/I(\omega_0 + \omega_n) \tag{48}$$

$$s(x_1) \triangleq \{I(\omega_n \psi_0 + \dot{\phi}_0) + x_1 \cos\alpha\}/I(\omega_0 + \omega_n) \tag{49}$$

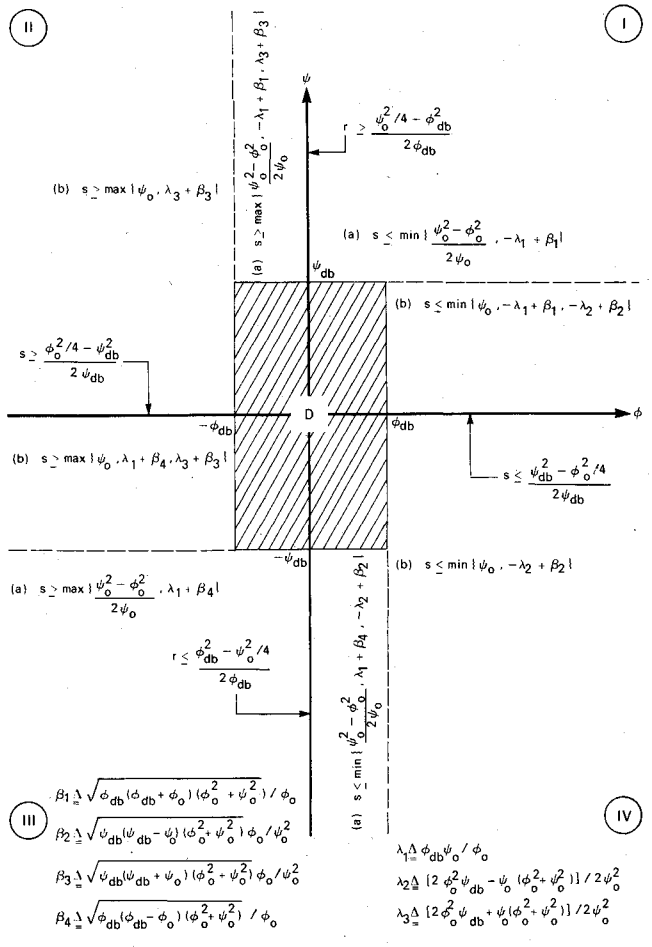

Fig. 5 Equivalent constraints on (r,s) due to bounds on attitude errors.

Furthermore, (r,s) must satisfy Eq. (28), which relates r and s through the expression

$$\phi_0 r + \psi_0 s = \tfrac{1}{2}(\phi_0^2 + \psi_0^2)$$

From this, the trajectory bounds (46) may be converted into an equivalent set of inequalities on either r or s which, through Eqs. (48) and (49), yield the necessary constraints on x_1 and x_3. The process is tedious but straightforward and is detailed in Ref. 10. A summary of these inequalities is shown in Fig. 5.

If we denote the control torque impulses that satisfy the attitude bounds (46) by the set

$$G \triangleq \{(x_1,x_3):\ r(x_1,x_3) \text{ or } s(x_1) \text{ satisfies the appropriate constraints in Fig. 5}\} \tag{50}$$

then the attitude error constrained DND solutions are given by the set $K \cap G$.

The constrained DND solutions of interest are then contained in the set $K \cap H \cap G$. Note that this set can nevertheless still be infinite or even empty. In the latter case, a constrained DND solution does not exist.† Henceforth, we will consider only the nonempty case. In particular, we seek a constrained DND solution which is optimal in the minimum-fuel sense.

†The existence of constrained DND solutions is a question that should not be lightly dismissed even though intuitively it is believed to be generic (i.e., a solution almost always exists). However, a rigorous proof is still pending.

Optimal Deadbeat Nutation Control

In spacecraft control problems, the DND solution that is of particular interest is one that minimizes the total control fuel. The latter is proportional to the total torque impulse generated by the control thrusters, which, in this case, may be described by the function

$$J(x_1,x_3,x_1',x_3') = \tfrac{1}{2}(x_1^2+x_3^2+x_1'^2+x_3'^2) \quad (51)$$

By Eqs. (39) and (40), this can also be written as

$$J(x_1,x_3) = (x_1-\tfrac{1}{2}a_1)^2+(x_3-\tfrac{1}{2}a_3)^2+\tfrac{1}{4}(a_1^2+a_3^2) \quad (52)$$

We can now define an *optimal DND solution* as one that minimizes J subject to the attitude and impulse constraints discussed previously. In other words, the problem is to find

$$\min_{(x_1,x_3)\in K\cap H\cap G} \quad J(x_1,x_3) \quad (53)$$

Since J is quadratic and K describes a straight line in the (x_1,x_3) plane, unless the set $K\cap H\cap G$ is empty, the optimal DND solution must be either a point on the boundary of $K\cap H\cap G$ [denoted by $B(K\cap H\cap G)$] or the unconstrained optimal solution (x_1^*,x_3^*) obtained via

$$\min_{(x_1,x_3)\in K} \quad J(x_1,x_3)$$

It is easy to show that (x_1^*,x_3^*) is given by

$$x_1^* = (a_1d^2+2cf-a_3cd)/2(c^2+d^2) \quad (54)$$

$$x_3^* = (a_3c^2+2df-a_1cd)/2(c^2+d^2) \quad (55)$$

It is clear that when $(x_1^*,x_3^*)\in K\cap H\cap G$, is is also the constrained optimal DND solution. Otherwise, the optimal solution must reside in the set $B(K\cap H\cap G)$, and can be obtained via

$$\min_{(x_1,x_3)\in B(K\cap H\cap G)} \quad J(x_1,x_3) \quad (56)$$

The advantage of this formulation over Eq. (53) is that the search is now restricted to the set $B(K\cap H\cap G)$ which contains a finite number of points. These points may be computed from Eq. (34) by replacing the inequalities involved in H and G with equalities.

We summarize with the following algorithm:

Step I (first impulse):

1) Measure $\{\phi_0,\psi_0,\dot{\phi}_0,\dot{\psi}_0\}$.
2) Compute parameters $\{a_1,a_3,c,d,f\}$ from Eqs. (35-37), (39), and (40).
3) Compute the unconstrained optimal solution (x_1^*,x_3^*) from Eqs. (54) and (55).
4) Check constraints: If $(x_1^*,x_3^*)\in G\cap H$, then it is also the optimal constrained solution; proceed to Step II. Otherwise, find

$$\min_{(x_1,x_3)\in B(K\cap H\cap G)} \quad J(x_1,x_3)$$

Step II (second impulse):

1) Compute (t^*,x_1',x_3') from Eqs. (38-40).

An estimate of the total number of algebraic operations incurred in the algorithm has been made in Ref. 10, and is summarized in Table 1. Here the off-line computations do not require attitude or rate information and can be prestored and updated periodically when necessary.

Some typical computation times for the major arithmetic operations are shown in Table 2. The figures quoted here are for implementation with a 16-bit 2's complement fixed-point arithmetic subroutine package operating on a (RCA) CDP 1802 COSMAC (8-bit) microprocessor system. The operations are performed in double precision, although single precision may also be used on a 16-bit processor at about one-third the computation time. Further reduction in computation time may be realized by utilizing hardwired multiplication.

Table 1 Computational requirements of the constrained optimal DND algorithm

Operation	Number of operations		
	Off-line	On-line	
		Best case	Worst case
+	2	17	59
−	1	16	49
×	3	41	85
÷	4	13	20
sin	1	...	...
cos	1	...	...
$\tan^{-1}$	...	2	2
$\sqrt{}$	1	2	2
min(max)	...	1	13
Ineq.	...	13	33

Simulation Results

The performance of the optimal DND control was evaluated via digital simulation of the dynamics of a CTS-type spacecraft with the following parameters:

I_1 = 1327.28 kg-m^2 (nom.)

I_3 = 1453.37 kg-m^2 (nom.)

h = 20 N-m-s

ω_0 = 0.0000727 rad/s

α = 10 deg

x_{1m} = 0.0026 N-m-s

x_{3m} = 0.0096 N-m-s

The dynamics simulated were those of the nonlinear Euler's equations of motion. Only the roll and yaw responses were of interest, although the pitch dynamics were also simulated. In addition, the effect of the rotating solar arrays on the moments-of-inertia was also included.

Figure 6 shows the capture responses for two sets of initial conditions:

$\phi_0 = 2.5$ deg $\quad \psi_0 = -2.5$ deg

$\dot{\phi}_0 = -0.1$ deg/s $\quad \dot{\psi}_0 = 0.1$ deg/s

and

$\phi_0 = 2.5$ deg $\quad \psi_0 = -2.5$ deg

$\dot{\phi}_0 = 0.1$ deg/s $\quad \dot{\psi}_0 = -0.1$ deg/s

The dependence of deadbeat time on the initial condition is typical of a nonlinear control system.

Figure 7 shows the response in the presence of impulsive disturbance torques. The deadbands were nominally set at $\phi_{db} = 0.012$ deg, $\psi_{db} = 0.1$ deg. The disturbance torques selected (50 ms pulses at 3% duty cycle) were considered to be typical during north/south stationkeeping. Only yaw disturbance (0.045 N-m) was present; the result with roll disturbance was similar and is not shown here.

Table 2 On-line computation times (in milliseconds)[a]

Operation	Best case	Worst case
+	1.156	4.012
−	1.248	3.822
×	52.89	109.65
	(5.904)[b]	(12.24)
÷	23.14	35.6
Total	78.434	153.084
	(31.448)	(55.674)

[a] Figures based on worst-case estimates for arithmetic functions on the CDP 1802 COSMAC microprocessor: add = 0.068 ms (16-bit 2's complement); subtract = 0.078 ms (16-bit 2's complement); multiply = 1.29 ms (16-bit 2's complement, 32-bit products); divide = 1.78 ms (32-bit 2's complement, 16-bit quotient and remainder).
[b] Parentheses denote hardware multiplication (0.144 ms/operation).

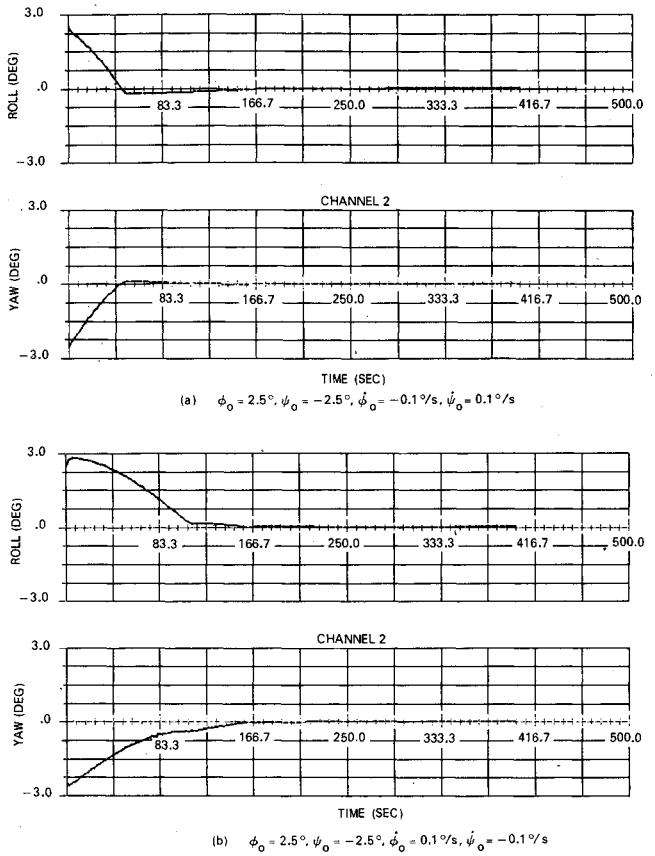

Fig. 6 Deadbeat nutation control responses.

Finally, the long-term performance of the controller was evaluated by extending the simulation to one full orbit (24 h). The deadbands were again set at ±0.012 deg for roll and ±0.1 deg for yaw. A periodic (at orbit rate) solar torque was also included. The results for different values of the solar torque amplitude are summarized in Table 3. The attitude trajectory for the 8-μ N-m case is shown in Fig. 8.

A good indication of the fuel consumption is given by the total control thrust impulse expended. Based on a specific

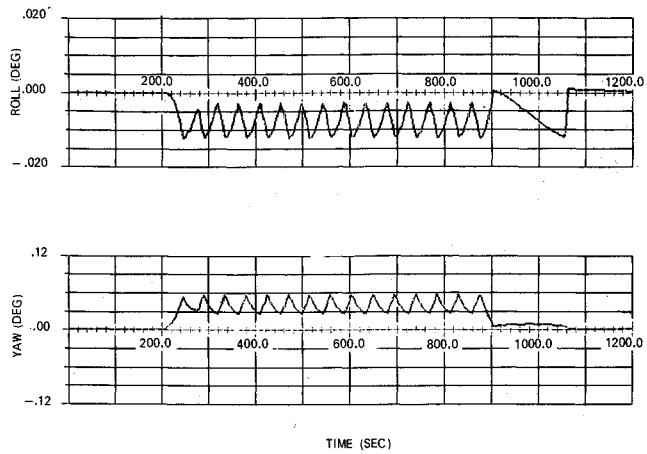

Fig. 7 Controlled nutation responses in the presence of disturbance torques.

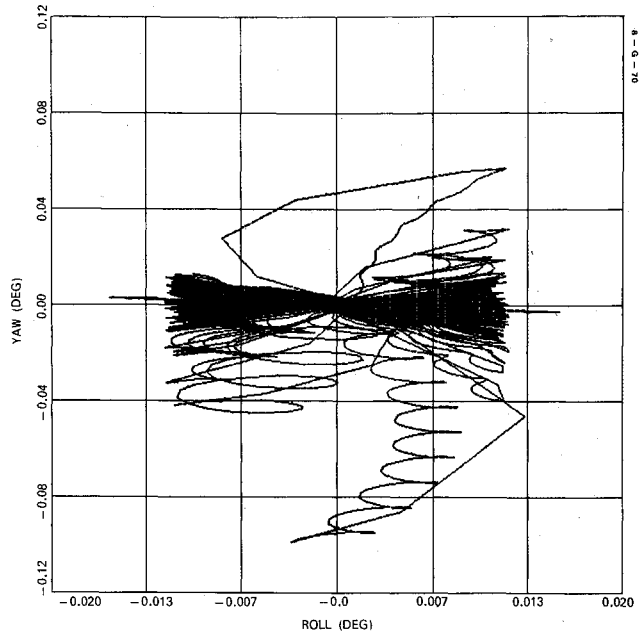

Fig. 8 On-orbit performance: solar torque amplitude = 8μ N-m.

impulse of 1960 N-s/kg, the total fuel required by the offset and yaw thrusters in the worst (8-μ N-m solar torque) case is about 3.1 kg/yr, which is appreciably higher than the amount consumed by the offset thrusters (0.27 kg/yr) on the CTS.[4] This is, however, to be expected of a control system whose accuracy is an order of magnitude higher than that of the CTS.

Conclusions

We have proposed a general procedure for achieving deadbeat nutation damping in two control impulses. The procedure reduces to the solution of a simple algebraic equation. An algorithm is obtained which results in optimal

Table 3 Summary of simulated on-orbit performance

Solar torque amplitude, N-m	Pulse counts/day				Thrust impulse/day, N-s	
	Offset		Yaw			
	Pos.	Neg.	Pos.	Neg.	Offset	Yaw
0.0	1	1	1	1	0.4217	0.0239
1.36×10^{-6}	18	18	18	18	2.4255	0.4524
8.14×10^{-6}	106	107	107	107	15.3946	1.3878

deadbeat nutation damping by minimizing the total control torque impulse subject to constraints on the impulse size and bounds on the attitude errors.

The deadzone, which is arbitrarily defined in the algorithm, essentially determines the control accuracy. In principle, any degree of accuracy may be specified. However, practical considerations such as fuel usage and sensor noise will eventually limit the accuracy that is achievable in any application. Our simulation results have demonstrated well the need for trade-off considerations between fuel consumption and pointing accuracy. The performance of the controller in the presence of sensor noises has yet to be studied.

A preliminary estimate of the computational requirements indicates that the control algorithm may in principle be implemented without difficulty on the present generation of microprocessor systems. The computational delays incurred are insignificant relative to the typical nutation period of the present day spacecraft; their stability impact on the attitude control loops is expected to be minimal.

The design flexibility of the algorithmic approach far surpasses that of the conventional pseudorate controller. For instance, it may be possible to modify the control accuracy of a spacecraft during flight as a means of fuel rationing under certain failure situations. With appropriate refinements, the methodology proposed here will serve well towards the development of a "general purpose" controller that is programmable for use in spacecraft designed for different applications.

Acknowledgments

The author would like to thank his colleague L.D. Morrow for his contributions to the simulation results. The work for this paper was performed with the sponsorship of the Communications Research Centre, Department of Communications, Ottawa, Canada, under the DSS Contract 07SU.36001-8-4258, S/N OSU78-00303.

References

[1] Dougherty, H.J., Scott, E.D., and Rodden, J.J., "Analysis and Design of WHECON—An Attitude Control Concept," AIAA Paper 68-461, AIAA 2nd Communications Satellite Systems Conference, San Francisco, Calif., April 8-10, 1968.

[2] Scott, E.D., "Pseudorate Sawtooth-Pulse-Reset Control System Analysis and Design," *Journal of Spacecraft and Rockets,* Vol. 4, June 1967, pp. 781-785.

[3] Millar, R.A. and Vigneron, F.R., "Attitude Stability of a Pseudorate Jet-Controlled Flexible Spacecraft," *Journal of Guidance and Control,* Vol. 2, March 1979, pp. 111-118.

[4] Vigneron, F.R. and Millar, R.A., "Flight Performance of the Stabilization System of the Communications Technology Satellite," *Journal of Guidance and Control,* Vol. 1, Nov. 1978, pp. 404-412.

[5] Hsing, J.C., Ramos, A., and Barrett, M.F., "Gyro-Based Attitude Reference Systems for Communications Satellites," AIAA Paper 78-568, AIAA 7th Communications Satellites Systems Conference, San Diego, Calif., April 24-27, 1978.

[6] Garg, S.C., "Optimal Yaw Estimation for a Class of Communications Satellites," Paper 12.2, Optimization Days, Montreal, Canada, May 23-25, 1979; also in "A Proposed Yaw Sensing Concept for Geostationary Communications Satellites," Dynacon Associates, Thornhill, Ontario, Canada, Rept. No. 78-05-01, Aug. 1978.

[7] Yuan, J. S-C., "Attitude Estimation and Control of Satellites in Geosynchronous Orbit," Paper 12-3, VIII IFAC Symposium on Automatic Control in Space, Oxford, U.K., July 2-6, 1979.

[8] Staley, D.A., "System Design for a Two-Axis Biased Momentum Controller," Ancon Space Technology Corp., Thornhill, Ontario, Canada, ANCON-R.788, April 1979.

[9] Lebsock, K.L., "High-Pointing Accuracy with a Momentum Bias Attitude Control System," AIAA Paper 78-569, AIAA 7th Communications Satellite Systems Conference, San Diego, Calif., April 24-27, 1978.

[10] Yuan, J. S-C., "Minimum Energy Control of Nutation in a Momentum Bias System," Spar Aerospace Limited, Toronto, Canada, SPAR-TM.1702, March 1979.